IEEE Access
Multidisciplinary | Rapid Review | Open Access Journal

Received February 7, 2021, accepted February 24, 2021, date of publication March 2, 2021, date of current version March 11, 2021.

Digital Object Identifier 10.1109/ACCESS.2021.3063201

Pollution Flashover Under Different Contamination Profiles on High Voltage Insulator: Numerical and Experiment Investigation

ALI AHMED SALEM[1], (Member, IEEE), R. ABD-RAHMAN[1], (Member, IEEE), WAN RAHIMAN[2], SAMIR AHMED AL-GAILANI[2], SALEM MGAMMAL AL-AMERI[1], MOHD TAUFIQ ISHAK[3], AND USMAN ULLAH SHEIKH[4]

[1]Faculty of Electrical and Electronic Engineering, University Tun Hussein Onn Malaysia, Johor 86400, Malaysia
[2]School of Electrical and Electronic Engineering, Universiti Sains Malaysia, Penang 14300, Malaysia
[3]Faculty of Engineering, National Defence University of Malaysia (UPNM), Kuala Lumpur 57000, Malaysia
[4]School of Electrical Engineering, Faculty of Engineering, Universiti Teknologi Malaysia, Johor Bahru 81310, Malaysia

Corresponding authors: Wan Rahiman (wanrahiman@usm.my), R. Abd-Rahman (rahisham@uthm.edu.my), and Salem Mgammal Al-Ameri (salemawadh@uthm.edu.my)

This work was supported in part by the Ministry of Higher Education (MOHE) through the Fundamental Research Grant Scheme under Grant K301, in part by the University Tun Hussein Onn Malaysia, and in part by the Collaborative Research in Engineering, Science, and Technology (CREST) under Grant 304/PELECT/6050423/C121.

ABSTRACT This work aimed to study the influence of contamination profiles and humidity on flashover electrical characteristics of polluted insulators. Firstly, the flashover tests on cap and pin glass insulators under four pollution levels represented by salinity were conducted. Eight artificial contamination profiles based on the solid layer method have been modeled for the selected insulators. The numerical analysis has been used to determine the insulator electrical characteristics such as potential, electric field, and power dissipation under proposed contamination profiles using finite element methods (FEM). Next, the power dissipation has been simulated with consideration of thermal stress propagation in locations with high power. Finally, flashover voltage gradient tests have been conducted under various humidity and contamination profiles. The values of the flashover voltage gradient due to pollution were determined as the percentage of the value of the flashover voltage gradient in the clean condition which was identified as the reference point. The numerical model indicated that the initiation of arc generally occurs at area in which the electric field and power dissipation is maximum. It was also observed from experimental results that the flashover voltage gradient under different contamination profiles has different values depends on the location and dimension of the pollution region.

INDEX TERMS Polluted insulators, contamination profiles, flashover voltage gradient, numerical model, finite element method (FEM), power dissipation.

I. INTRODUCTION

The flashover phenomenon of contaminated insulators is one of the major concerns among power utilities which threatens the reliability of operation and transmission of power. Much consideration has recently been given to cup and pin insulators used both in distribution and transmission [1]–[3]. The high voltage outdoor insulators could be enveloped by a layer of pollutants that fly through the air. Once the pollution layer is subjected to moisture, rain, or fog the contamination layer becomes conducting which leads the flow of leakage current (LC) on the insulator surface to the ground terminal (towers). Under such conditions, the insulator contamination flashover might easily occur [4]–[6]. Insulator pollution is the first step to the flashover, whose mechanism is influenced by several dynamic variables such as the configuration of the insulation, pollution and the climate. Therefore, it remains important to pursue with more investigations in connection insulator pollution.

In recent years, several researches work on the deposition of pollution have been conducted [2], [7]–[11]. In report [2], the impact of distribution of pollutants on flashover voltage of various types of insulators were analyzed in a uniform method. It was observed that the flashover voltage

The associate editor coordinating the review of this manuscript and approving it for publication was Ananya Sen Gupta.

has a greater effect on composite insulators than on porcelain insulators under uniform contamination. Non-uniformity of contamination has been investigated on the bottom and top [7], along the insulator leakage distance [8], or fan-shaped [9], [10]. As per [7], the flashover voltage stress of the glass and porcelain insulator strings is reduced by raising the non-uniformity level of the fan-shaped non-uniform pollution. According to [9], a huge influence in the flashover voltage (FOV) value was caused by the uneven pollution degree (bottom/top), which is about 28%–30% greater than the FOV with the uniform contamination. Authors in [11] have studied the effect of formation of dry band, its width and location on the FOVs and arc growth. It has been found that dry band formation can elevate the magnitude of FOVs and also promote the growth of arcs on wetted surfaces of insulators. The formation of dry bands was first studied by Hampton [12], which experimentally measured the voltage distribution along a contaminated insulation strip and identified a relationship between the voltage applied and the resistance of the dry band. To validate the Hampton criterion, authors in [13] gathered the crucial temperature and electrical field required to shape a dry band on a dirty insulator surface. They observed that the width of the dry band and its development depend on the volume of power dissipated inside the dry band.

The finite element method (FEM) was one approach to simulate the numerical models of the dry band effect. These models were used to describe the dry band effect on the distribution of electric field and voltage on the insulators [14]–[17]. To date, tests of artificial pollution flashover for sample insulators (example: plate) have been conducted in order to evaluate the effect of humidity, dry band and non-uniform pollutions in different contamination profiles [18]. However, the pollution, humidity and dry band effects on flashover performance for real cap and pin glass insulators have not been reported yet. To the best of our knowledge, the effect of simultaneous presence of uneven wet contamination, multi-dry band, and pollution location, as a worst-case scenario, on the flashover voltage of glass insulators is still unknown.

This paper focuses on assessing the effect of distribution of pollution, humidity and dry band dimension and location on the flashover voltage of glass insulator. Eight proposed contamination profiles were established as shown in Figure 1. Each contamination profile has different conditions according to pollution and dry band locations. AC contamination flashover tests of cup-pin glass insulator were carried out in a chamber room. During the experiments, the specific degree of contamination was emulated by an artificial process. The pollution flashover voltage gradient values were calculated as the percentage of the flashover voltage gradient value in the clean state that was defined as a reference point. Then the polluted glass insulator was simulated using FEM according to the proposed contamination profiles.

In this paper, the preparation of the test sample and experiment produce were discussed in Section 2. Section 3 introduces the effect of the proposed scenarios pollution distribution and humidity on flashover voltage gradient

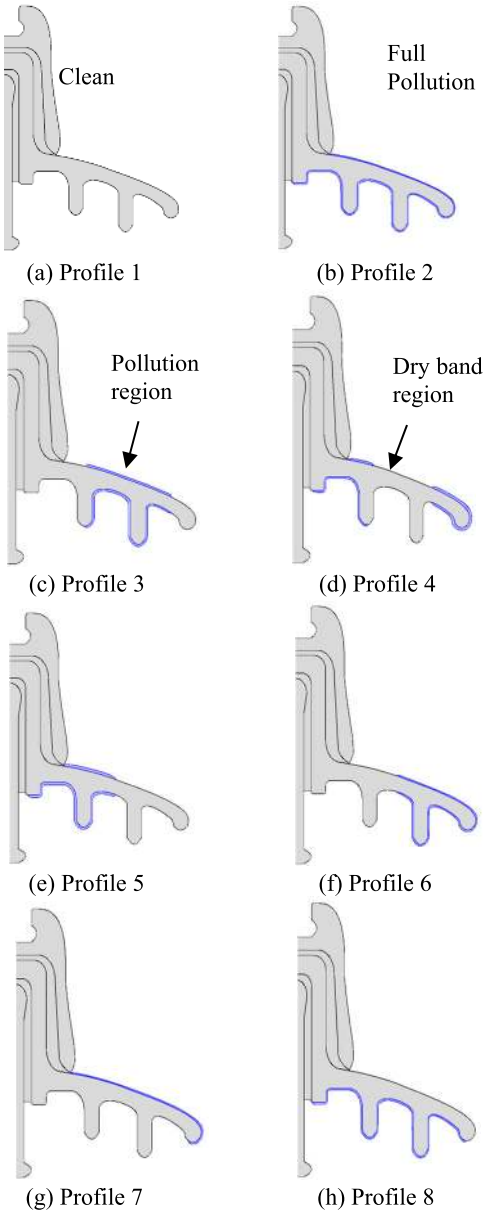

FIGURE 1. The proposed contamination profiles.

performance. In Section 4, the numerical model based on FEM is described. In addition, potential, electric field, and power dissipation distribution results were displayed. Finally, the conclusion of the study and future work are reported in Section 5.

II. NUMERICAL APPROACH

A. FEM MODEL AND PARAMTERS

In this study, the finite element method (FEM) has been utilized to simulate the potential voltage and electric field distribution along an insulator. COMSOL Multiphysics 5.5 software is adopted particularly to perform analysis processes. The potential, electric field and power dissipation computations are quasistatic, they can be calculated by the electrostatic module. The electrostatic solver under AC/DC

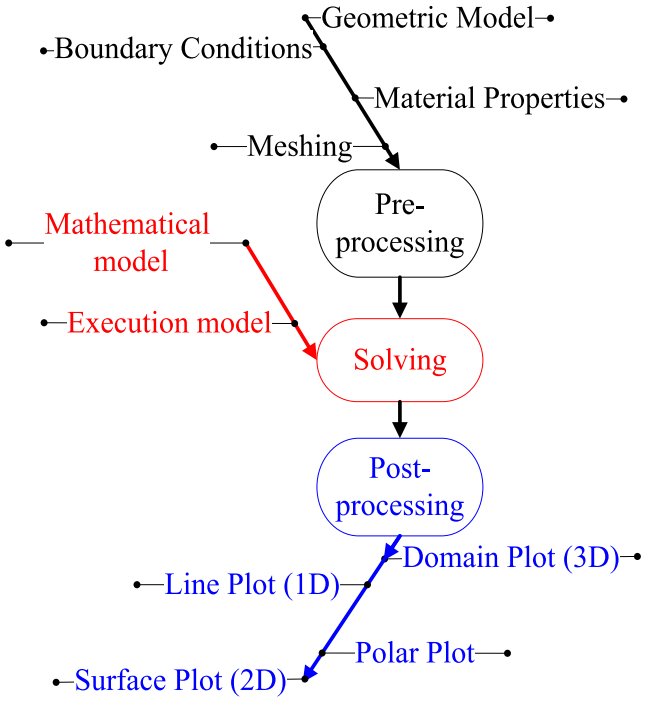

FIGURE 2. COMSOL multiphysics finite element method (FEM) procedure.

physics formulation was used for all simulations. The insulator under test implemented with the proposed contamination profiles models are generated with a 2D modeler for simplicity. The mesh density is higher in the critical regions of the insulators where higher accuracy is required such as the corners. Solving FEM denotes the contours and surface analytics of the equipotential and the electrical field distribution on the insulator. The simulation process flowchart of FEM Figure 2. The glass insulator under clean and polluted conditions has been modelled. An amount of 11 kV of AC voltage is applied to the bottom of the insulator whereas the top of the insulator is connected to the ground. The electrical parameters, which are permittivity and conductivity value as listed in Table 1, are adopted for the FEM simulation. The pollution layer was assumed to be uniform at three different thicknesses listed in Table 2 on the insulator surface to replicate eight pollution profiles. The conductivity of the pollution layer for each pollution profile was adopted from those obtained from the actual laboratory measurements. Therefore, the simulation work was conducted in eight different contamination profiles of pollution distribution proposed in this study.

B. POTENTIAL AND ELECTRIC FIELD DETERMINATION

A direct parameter of determining the distribution of E- Fields (E) is gradient of electric potential (V) as [19]

$$E = -\nabla V \tag{1}$$

The electric potential has been calculated by

$$\nabla \cdot (\sigma \nabla V) + \frac{\partial}{\partial t} \nabla \cdot (\varepsilon \nabla V) = 0 \tag{2}$$

TABLE 1. Properties of insulator materials.

Types of material	Relative electric permittivity	Electric conductivity in COMSOL
Air	1	0
Cement	15	10^{-4}
Pollution layer	81	10^{-3}
Insulator (glass)	4.2	0
Insulator cap	1000	5.9×10^{7}
Insulator pin	1000	5.9×10^{7}

TABLE 2. Thickness of pollution layer.

Pollution level	Pollution layer thickness (cm)
Clean	None
Light	0.1
Moderate	0.15
Heavy	0.2

The change of E-Field can be calculated using Maxwell's expression,

$$\nabla E = \rho/\varepsilon \tag{3}$$

by substituting E previously defined in (1) into (3), the equation of Poisson has been obtained as,

$$-\nabla \cdot (\varepsilon \nabla V) = \rho \Rightarrow \nabla^2 V = -\rho/\varepsilon \tag{4}$$

When $\rho = 0$, Laplace's expression is obtained as

$$\nabla^2 V = 0 \tag{5}$$

where ε is the electric permittivity, σ is the electric conductivity and ρ is the resistivity. The distribution of potential in (r, z) based on Laplace is given by

$$\frac{\partial^2 V}{\partial r^2} + \frac{1}{r}\frac{\partial V}{\partial r} + \frac{\partial^2 V}{\partial z^2} = 0 \tag{6}$$

The function $F(v)$ of 2D in the coordinates Cartesian system has been defined as [20],

$$F(v) = \frac{1}{2}\iint \left[\varepsilon_r \left(\frac{dv}{dr}\right)^2 + \varepsilon_z \left(\frac{dv}{dz}\right)^2\right] drdz \tag{7}$$

When the distribution of permittivity is isotropic in r- and z-coordinates the $\varepsilon_r = \varepsilon_z = \varepsilon$ and the Equation (7) can be re-written as,

$$F(v) = \frac{1}{2}\iint \varepsilon \left|\nabla^* v\right|^2 ds \tag{8}$$

The contribution to the rate of change of F with V from the variance of the potential of node i in element e only, x_e, can be determined as:

$$x_e = \frac{dF(v)}{dv} = \frac{1}{2}\iint \left[\frac{\varepsilon}{dv}\left(\left(\frac{dv}{dr}\right)^2 + \left(\frac{dv}{dz}\right)^2\right)\right] drdz \tag{9}$$

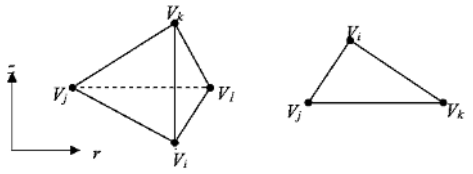

FIGURE 3. Typical finite element subdivisions of an irregular domain and typical triangular element.

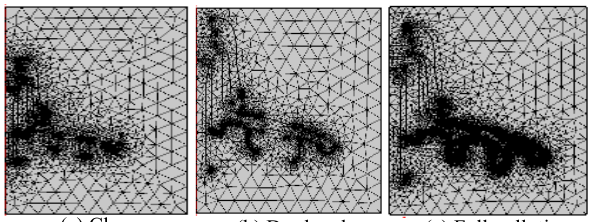

(a) Clean (profile 1) (b) Dry band (profile 4) (c) Full pollution (profile2)

FIGURE 4. Finite element method mesh results under normal size of element.

$$x_e = \frac{\varepsilon}{2}\iint\left[2\frac{dv}{dr}.\frac{d}{dv_i}.\left(\frac{dv}{dr}\right)+2\frac{dv}{dz}.\frac{d}{dz_i}.\left(\frac{dv}{dz}\right)\right]drdz \tag{10}$$

By considering the effect of pollution conductivity on the distribution of electric field, the Equation (7) is given by

$$F^*(v) = \frac{1}{2}\iint(\sigma + j\omega\varepsilon)\left|\nabla^* v\right|^2 ds \tag{11}$$

where ε is the electric permittivity, ε_r and ε_z are permittivity on r and z components, σ is the electric conductivity, v is the electric potential and ω is angular frequency. The electric potential of any arbitrary point inside each sub-domain is expressed as

$$v_e(x, y) = a_{e1} + a_{e2}x + a_{e3}y \tag{12}$$

In Figure 3, the electric potential at every node in the total network composed of many triangle elements is calculated by minimizing the function $F(v)$, as [21],

$$\frac{\partial F(v_i)}{\partial(v_i)} = 0, \quad i = 1,\ 2,\ 3.....,\ k \tag{13}$$

k presents the number of nodes in network. The final matrix is written as

$$[S_{ij}]^e\{v_i\}^e = \{q_j\}^e i, \quad j = 1, 2, ...k \tag{14}$$

Figure 4 shows the meshing of the insulator under clean, dry band, and full pollution conditions. The normal element size was selected in the meshing process for all scenarios. The simulation algorithms of the finite element approach are shown in the following flowchart given in Figure 5.

The mesh characteristics and number of degrees of freedom (DOF) solved for all scenarios are listed in Table 3.

The 2D FEM model is assigned with the material properties and boundary conditions as described above. The electric parameters used in this study are adopted into COMSOL Multiphysics software according to the model algorithm in Figure 5.

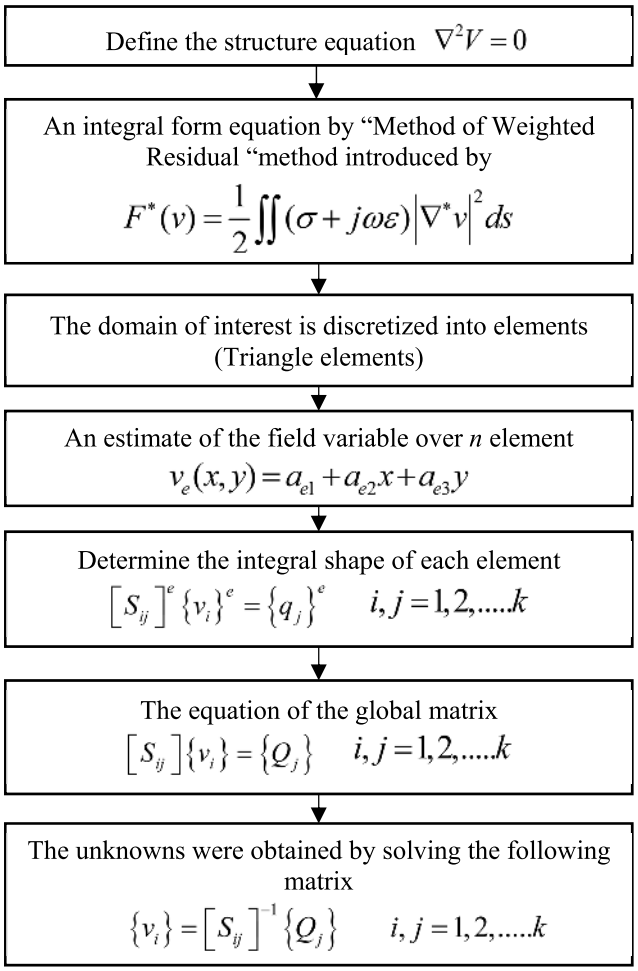

FIGURE 5. Finite element method algorithm.

TABLE 3. Domain elements and boundary elements numbers.

Profile Code	Elements Types			Minimum Elements Quality	DOF
	Triangle	Edge Element	Vertex Element		
A	7719	521	58	0.4807	15524
B	17634	1420	84	0.2147	35351
C	10604	770	71	0.4644	21297
D	9924	784	82	0.4517	19937
E	12593	979	75	0.4142	25278
F	11122	850	77	0.4802	22335
G	12040	889	67	0.358	24165
H	9491	781	79	0.4556	19066

C. SIMULATION RESULTS

Figures 6 and 7 show the potential and electric field distribution, respectively, along the glass insulator for all proposed contamination profiles. In a clean insulator, the electric potential reduces gradually from HV terminal to ground terminal. It is worth mentioning that the contour line pattern indicates the different potential values across the insulator. The potential distribution in a clean insulator is non-linear because of the capacitive effect of a clean surface. While in a polluted

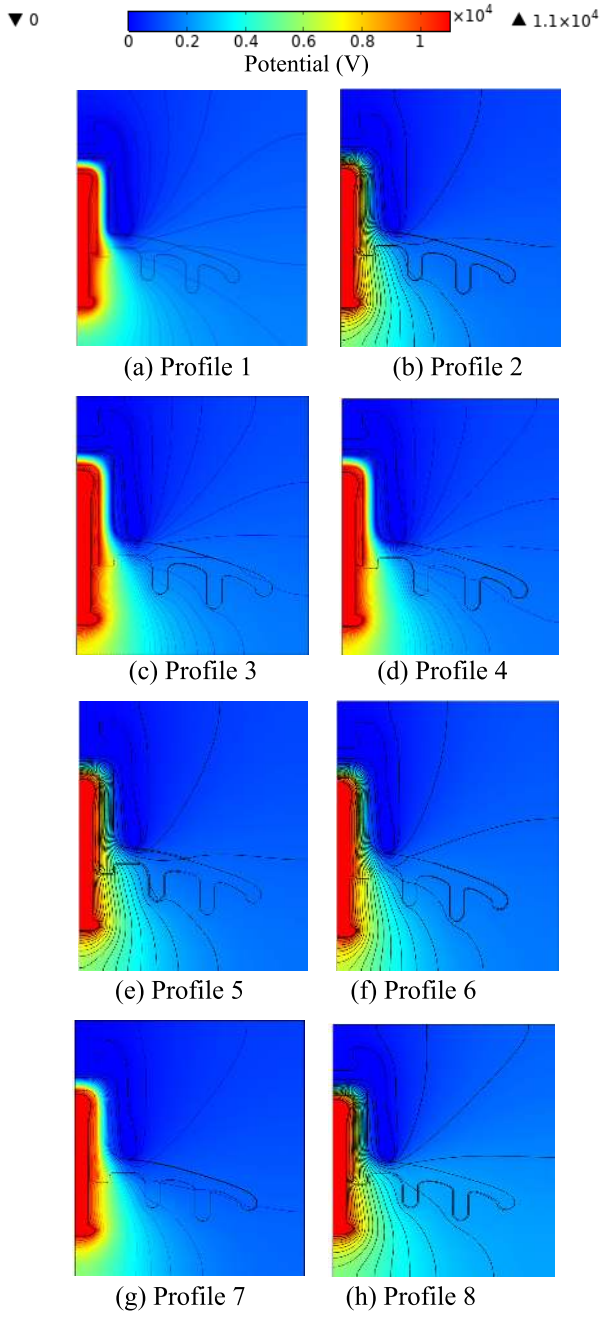

FIGURE 6. 2D Potential distribution on insulator surface for all pollution Profiles.

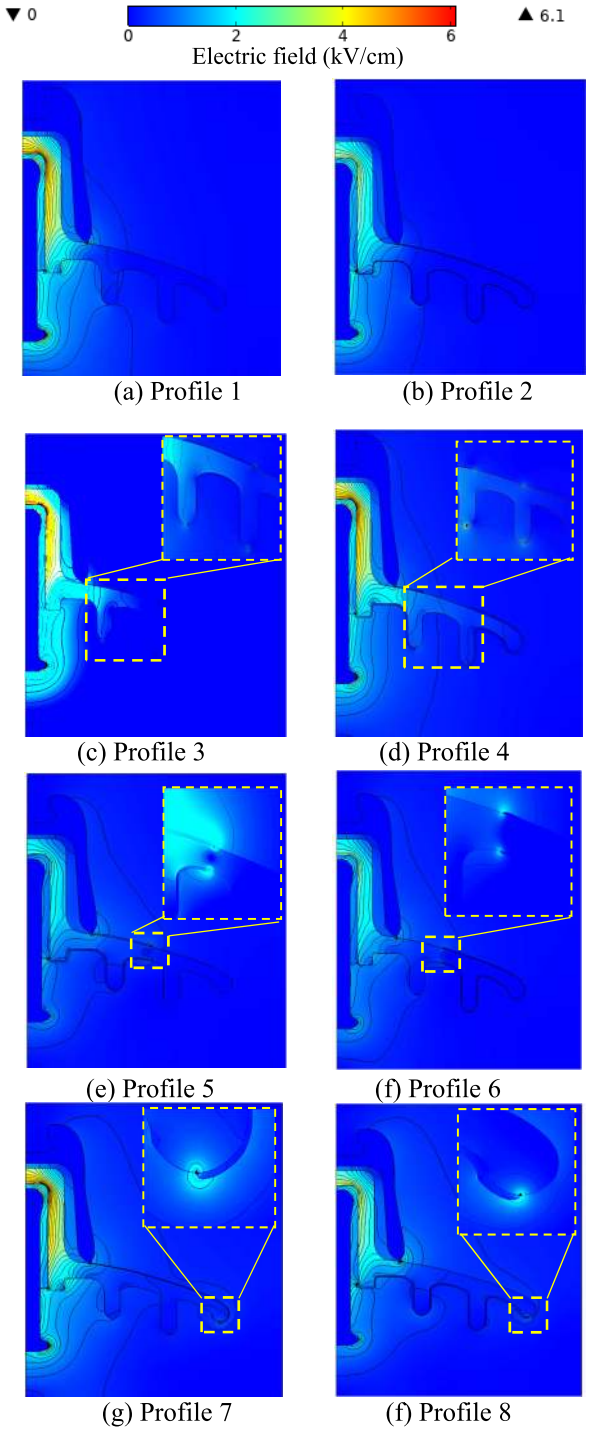

FIGURE 7. E-Field distribution on insulator surface for all pollution profiles.

insulator the potential distribution depends on the contamination severity and dry band properties.

For electric field distribution, the maximum values of strength of the electrical field were observed inside the insulator material (glass) between the pin and cup and the nearby region of insulator HV electrode and then around the ground pole because of the charge accumulated in the poles. Furthermore, it has been accepted in Figure 6 that the potential line density shows the concentration inside and around the high voltage pole of the insulator.

Minimum E-Field was seen at the end of the shed area, where the electrical charges are almost non-existent in this region. Other than that, the distance of equipotential lines for each of the contamination profiles is also different. As can be seen from Figure 7, the equipotential lines become wider in the less polluted condition compared to other polluted conditions. The wider distribution of equipotential lines

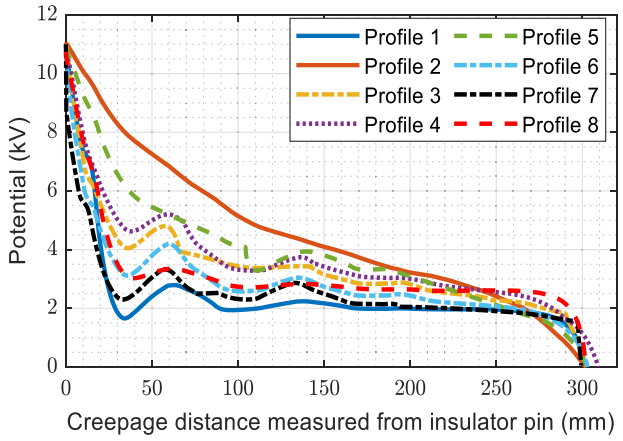

FIGURE 8. Potential distribution along insulator leakage distance for all pollution profiles from HV to ground.

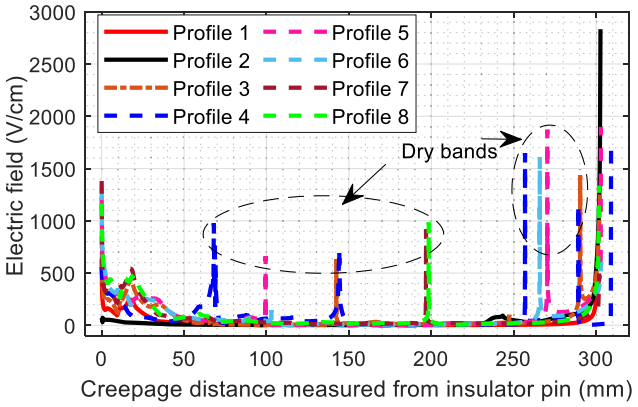

FIGURE 9. E-Field distribution along insulator leakage distance of studies contamination profiles.

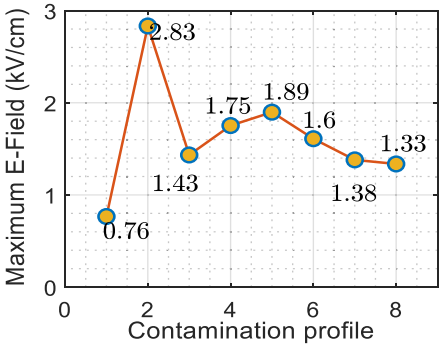

FIGURE 10. Maximum E-Field value at each contamination profile.

in top-polluted insulators indicates that the insulators have lower intensity of the electric field. It can be concluded that the present of contamination can decrease the electric potential across the insulator. According to an investigation conducted by [22], the electrical properties can be enhanced with the addition of pollution on the insulator surface which may also increase the breakdown voltage. The charge formation is related to the existence of conductivity variation on the insulator surface. The variance in conductivity leads to interfacial polarization occurrence and encourages charge accumulation in the cross point of pollution with the insulator that results in the presence of an electric field high value on both sides of the dry bands as seen in the zoom box in Figure 7.

The potential distribution along leakage distance of the insulator for proposed contamination profiles is completely different as shown in Figure 8. According to Figure 8, it can be seen that the electrical potential of the insulator decreased sharply under clean condition from 11 to 1.8 kV along 35 mm from leakage distance. Then, the voltage fluctuates at 160 mm and subsequently remains about 2 kV until 290 mm and then declines to 0 kV. Whereas, the voltage of a full polluted insulator (profile 2) decreased gradually from 11 kV to 0 V. The decrease in voltage in the proposed contamination profiles depends on dry band location, where the dry band which is near the ground terminal has a less sharp decrease compared to high voltage terminal. It can also be inferred that the distribution of potential gradually approaches the linear distribution under heavy polluted cases. The density of E-field increases as the conductivity of the contamination layer rises and the largest E-Field was noted in the condition of severe pollution (profile 2 of 2879 V/cm) as shown in Figure 9.

The formation of dry bands at the surface of the insulator is a very important issue that needs to be considered when investigating the insulators. Literature has shown that the flashover of insulators is highly affected by dry bands formation. Therefore, eight proposed contamination profiles with different locations for dry band were considered. The maximum values of E-Field are figured in Figure 10. According to Figure 10, the maximum value of E-Field in the contamination profile 2 (full pollution) contributes to the greatest extent followed by contamination profiles 5, 4, 6, 3, 7 and 8. This indicates that the dry band formation in the middle of the pollution layer leads to electric field intensification if compared to the other profiles, as in the case of profile 5. The electric field is also increasing with the increase in the dry band length, especially if the dry band is close to the high voltage end. In the case of dry band formation at the end of pollution layer, the electric field is intensification is slightly lower as shown in profiles 7 and 8.

The voltage distribution along the polluted insulator under different levels of insulator conductivity in case full pollution (profile 2) is demonstrated in Figure 11. The conductivity of the contamination layer was varied to compute light, moderate, and heavy contamination. It can be observed from Figure 11 that the voltage distribution in the case of heavy pollution seems linear. The voltage decreased with the decline in contamination severity. For light pollution, the distribution of voltage changes are negligible compared to the clean insulator. The shape and values of electrical potential are different due to the increase in pollution level. The highest change in potential value was in the inner rib. It can be seen that the electrical potential at 35 mm increases from 1.8 to 2.6, 5.8,

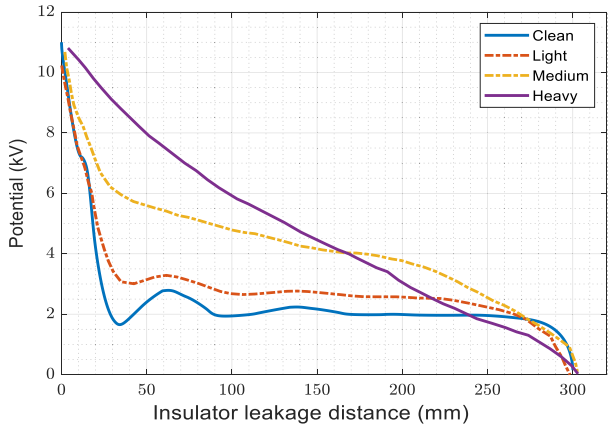

FIGURE 11. Voltage distribution for various pollution level.

and 9 kV when the contamination level varies from clean to light, medium, and heavy, respectively.

D. POWER DISSIPATION EVALUATION

The parameter most affected by the presence of a moist pollution layer on the insulator surface is the leakage current (LC). The leakage current causes the power dissipation in the contamination layer, results in the resistant heating of the contamination film layer, which causes the moisture to dry out and the formation of dry strips on the insulator surface. At any region along leakage distance of insulator, the power dissipation in contamination film of thickness, t, is proportional to the contamination film resistance and the LC magnitude, I. The total power dissipation formula given as:

$$P = R_P \cdot I^2 \tag{15}$$

The power dissipation as a function of parameters of the insulator is formulated as:

$$P = 2\pi rl\sigma E_t^2 t \tag{16}$$

where R_p, l, A, and σ are the resistance, length, area of a small section from the insulator, and conductivity of the contamination layer. While r represents the insulator radius. Using $S = 2\pi rl$ to represent the insulator area, the power dissipation can be obtained in the contamination film per unit surface area along leakage distance as:

$$P_a = P/S = \sigma E_t^2 t \tag{17}$$

The power dissipation per contamination film volume is written as

$$P_v = P_a/t = \sigma E_t^2 \tag{18}$$

Equations (17) and (18) are used to estimate the power dissipation on outdoor insulators, then, to facilitate the forecast of formation of dry bands on the insulator surface. Figure 12 shows the surface power dissipation of the proposed contamination profiles under medium contamination and 75% humidity. The power dissipation has been calculated using (17) within the COMSOL software.

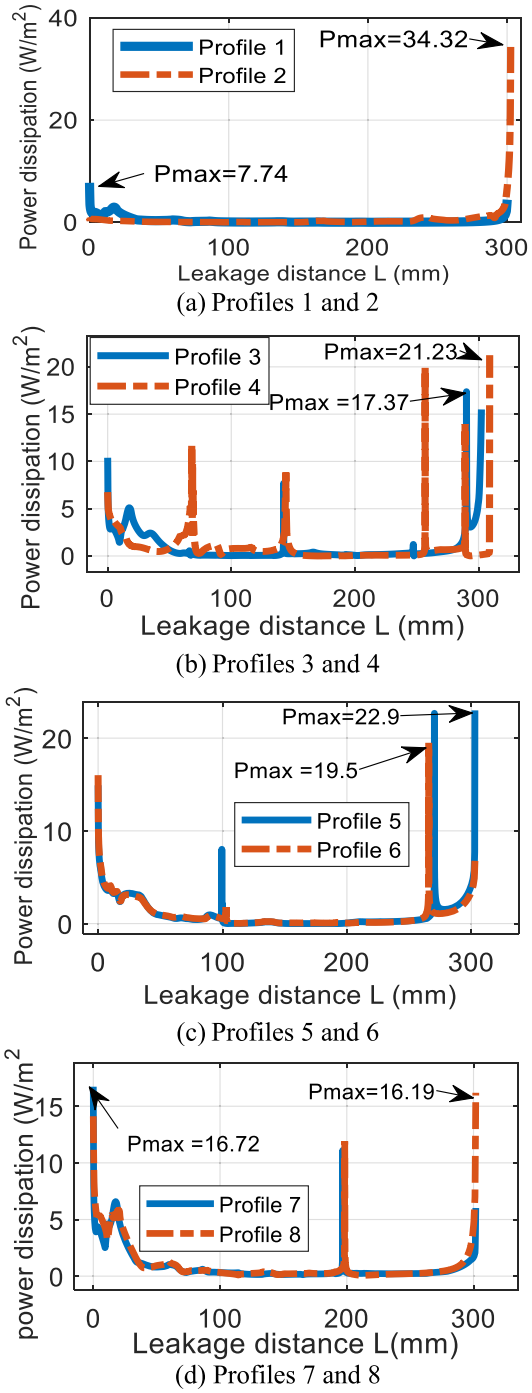

FIGURE 12. Power dissipation along insulator for proposed contamination profiles.

III. EXPERIMENTAL WORK

A. TEST SAMPLE PREPARATION

In this work, a cap and pin glass insulators were used. Its geometrical profile and specifications are given in Figure 15 and Table 4, respectively. The insulator has been polluted artificially with four different levels of salt solution, i.e., 20 g, 40 g, 80 g and 100 g of sodium chloride which dissolved in 1 l of distilled water to produce 0.05, 0.15, 0.25, and

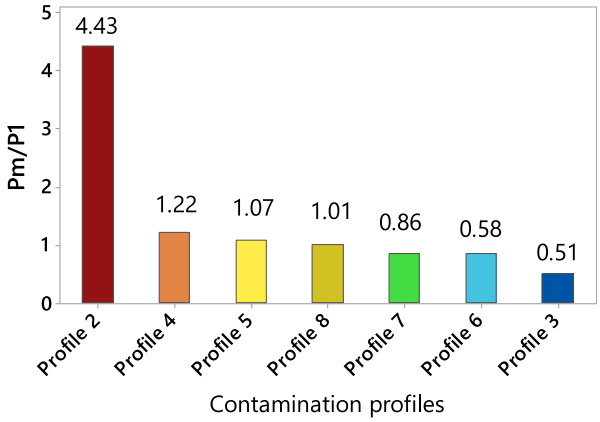

FIGURE 13. Contaminated profiles (Pm)/ clean profile 1 (P1) of proposed contamination profiles.

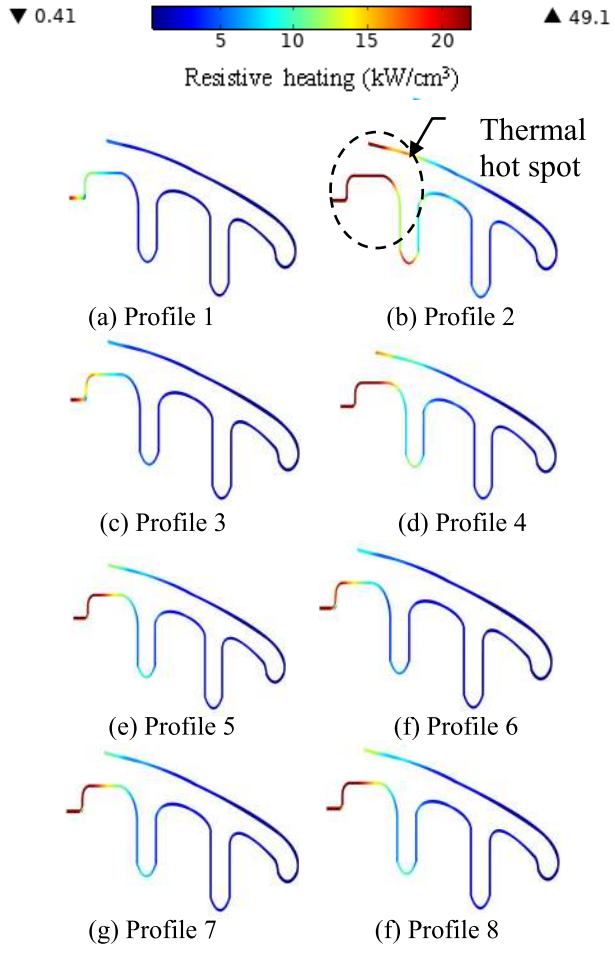

FIGURE 14. Power dissipation per unit volume for all contamination profiles.

0.35 mg/cm2 salt deposit density (SDD), respectively. The contamination was applied on the surfaces of the insulators based on solid layer method uniformly [23]–[28]. The test specimens were sprayed using the prepared suspension and were left to dry naturally at room temperature for 24 h before being suspended in the chamber. Sodium chloride salt (NaCl)

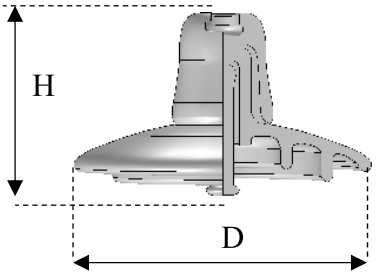

FIGURE 15. Schematic of the insulator profile adopted for study.

TABLE 4. Insulator parameters.

Parameters	Value (cm)
Insulator height H (cm)	14.6
Diameter D (cm)	25.5
Leakage distance L (cm)	32
Length of lower side L_L (cm)	20.5
Length of upper side L_u (cm)	11.5

and Kaolin were used to simulate the contamination layer. Equivalent salt deposit density (SDD) that would produce the defined conductivity has been selected to characterize the severity of polluted insulators. The conductivity, salinity and the SDD were determined by using the following equations, in accordance to the IEC60507 [29].

$$S_a = 5.7 \times (\sigma_{20})^{1.03} \tag{19}$$

$$SDD = (S_a \times V)/A \tag{20}$$

where σ_{20} is layer conductivity at 20 °C, A is insulator surface area, S_a is solution salinity in g/l, and V is solution volume in cm^3. The suspension conductivity has been measured by using a conductivity meter HI8733.

The salinity has a direct effect on the electrical conductivity of contaminated layers. Table 5 reveals the salinity, the conductivity and SDD values. The insulator was tested in clean and pollution conditions as shown in Figure 16.

The non-soluble deposit density (NSDD) was determined as:

$$NSDD = \frac{(w_f - w_i) \times 10^3}{A} \tag{21}$$

where w_f, w_i and A are the filter paper containing pollutants weight, the filter paper under dry conditions weight, and area insulator surface, respectively. The non-soluble deposit density (NSDD) has been estimated to be six times greater than the soluble deposit density (SDD).

B. TEST PROCEDURE

The test has been carried out in the UTHM high voltage laboratory. The laboratory test setup consists of a 0.230/100-kV, 5-kVA, 50-Hz transformer which provides a single-phase AC voltage up to 100 kV to energize the tested insulators. The capacitive divider was used to measure the flashover voltage.

TABLE 5. Salinity, ESDD and conductivity.

Salinity (g/l)	ESDD (mg/cm2)	Conductivity (μS/cm)	Contamination severity
20	0.052	503.47	Light
40	0.167	1698.28	Medium
60	0.242	2654.71	Heavy
80	0.363	3845.96	Very Heavy

(a) Clean (b) Pollution

FIGURE 16. Clean and polluted glass insulator.

Figure 17 shows the experiment setup and pictorial view of the flashover voltage measurement system.

The insulator sample was suspended in a chamber room, consisting of 50 × 50 × 125 cm polycarbonate sheet walls. The flashover voltage gradient, E_c measurements were conducted under humidity of 75%, 85%, and 95% controlled by fog generator per each degree of contamination. For each specified level of humidity and pollution, a voltage rise of 2 kV/sec and flashover measurements were conducted four times with intervals of three minutes to prevent the effect of present flashover on the subsequent measurement. The average flashover voltage, U_F(kV) and its relative standard deviation error (σ %) of 4 tests for each point were calculated by the following expressions [30]:

$$U_F = \frac{\sum (U_i n_i)}{N} \tag{22}$$

$$E_c = \frac{U_F}{L} \tag{23}$$

$$\sigma\% = \frac{\sqrt{\left(\sum_{i=1}^{N} (U_i - U_F)^2\right)/(N-1)}}{U_F} \times 100 \tag{24}$$

where U_i, n_i, N and L are the applied voltage, number of tests which were conducted at U_i and number of valid tests and insulator length, respectively.

IV. EXPERIMENTAL RESULTS

A. FLASHOVER VOLTAGE PERFORMANCE UNDER DIFFERENT POLLUTION PROFILES

Figure 18 shows the flashover voltage gradient results of the proposed contamination profiles for the deposit of pollutants and the location of the dry bands under various humidity conditions for the polluted insulator. The measured flashover voltage gradient of the insulator under clean conditions is 1.36 kV/cm. This value has been considered as a reference

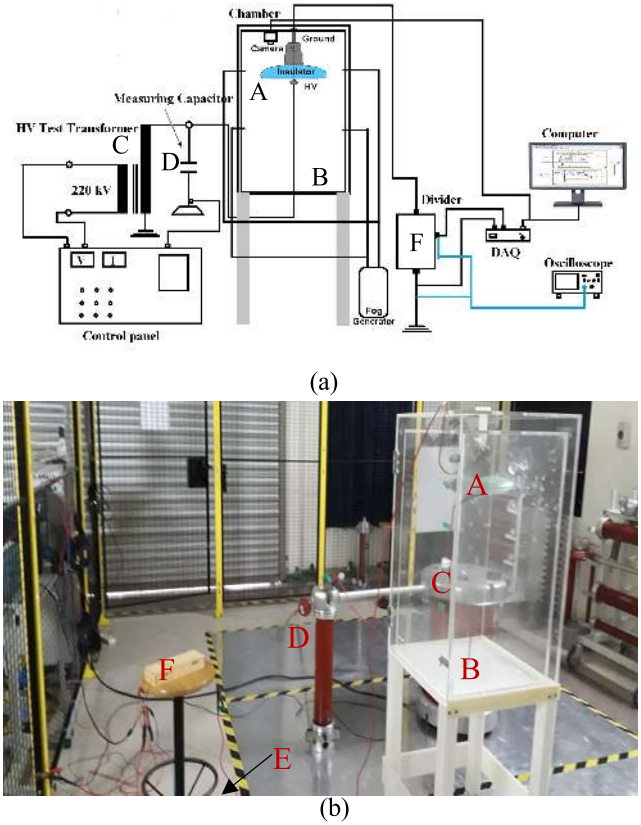

FIGURE 17. (a) Schematic diagram of the experiment setup (b) The pictorial view of the setup. Component labels: A: the tested samples, B: chamber, C: transformer, D: capacitor, E: fog generator and F: potential divider.

value to analyze the pollution severity and dry bands location effect on flashover voltage gradient E_c. Under pollution conditions, the insulators' flashover voltage gradient value dropped sharply when compared to clean conditions. From Figure 18, for all contamination profiles, it can be seen that the Ec of insulator gradually reduces with increasing salinity (pollution severity). This implies that the relationship between the flashover voltage gradient and the salinity has a negative power function as defined in (24) extracted from the fitting of the results [31], [32]

$$E_C = x(S_a)^{-y} \tag{25}$$

where x is a constant that depends on the profile and materials of the insulator and humidity. While y is the characteristic indicator of contamination on the insulator. The coefficient R^2 is more than 0.95 for all pollution profiles, therefore, the fitting rate expressed in (24) is satisfactory. It should be remembered that the higher the voltage gradient value of the flashover, the better the condition of the insulator. In Figure 18a, the variations in the flashover voltage gradient versus salinity humidity of 75% for contamination profiles 1 and 2 are shown. It can be seen that by increasing salinity from 20 to 40, 60 and 80 g/l, this has resulted in corresponding decreases in Ec from 0.71 to 0.45, 0.33 and 0.26 kV/cm, respectively. The percentage of Ec value

to the reference value of 1.36 kV/cm (Ec at clean condition) decreased by 52.17%, 33.13%, 24.71% and 19.6% with increasing salinity from 20 to 40, 60 and 80 g/l, respectively. The $E_c - S_a$ curve in contamination profiles 3 and 4 are shown in Figure 18b. The flashover voltage gradient reduces gradually with the rise of salinity. It can be concluded that the relative deviation error for all tests is lower than 5.6%. This means the dispersion rate of flashover voltage is acceptable, which implies that the approach used in the experiments is reasonable.

From Figure 18b, with increasing the salinity amount from 20 to 40, 60 and 80 g/l for glass insulators under distributed pollution, the Ec is lessened approximately 27.17% to 50% in contamination profiles 3 and 4. Comparing contamination profile 3 and profile 4 in Figure 18b, it can be observed that the influence of increasing salinity in profile 4 is more serious than the influence of increasing salinity in profile 3 on the Ec under the same conditions. Thus, the location of accumulation of the contamination impacts the flashover creation on polluted insulator surfaces. As for E_c in Figure 18c, the value decreases with increasing contamination severity (salinity) under inner ring and outer ring pollution (profile 5 and profile 6). In contamination profile 5, the percentage of flashover voltage gradient E_c value to reference value decreased by 56.9%, 38.7%, 30.5% and 25.2% with increased salinity from 20 to 40, 60 and 80 g/L. Whereas in profile 6 (inner ring pollution), the flashover voltage gradient percentages of the insulator are 54%, 34.9%, 26.9% and 21.8% with salinity of 20, 40, 60 and 80 mg/cm2, respectively. Comparing profile 5 and profile 6, it can be noted that the E_c percentage in profile 5 is more than the E_c percentage in profile 6 at the same pollution level.

This indicates the pollution in the inner ring surface of the insulator (High Voltage (HV) side) is more serious than in the outer ring surface.

Figure 18d represents the E_c and salinity relation curve for the insulator in the top (profiles 7) and bottom (profiles 8) surface. According to the result in Figure 18d, by increasing the salinity from 20 to 40, 60 and 80 g/L under profile 7, the E_c dropped 34%, 52.7%, 61.8% and 69.2%, while in profile 8 E_c decreased by 39.5%, 56.4%, 65.2% and 73.3% respectively. Results indicate that the flashover voltage gradient E_c in the bottom pollution case is considered the lowest in comparison with top pollution profile. The percentage of E_c values to reference value for all contamination profiles under salinity levels and humidity of 75% is shown in Figure 19.

The effective range for each contamination profile under humidity of 75% and salinity between 20 and 80 g/l on flashover voltage gradient has been quantified by using the box plot. The box plot shows the Q (0.25), Q (0.5), and Q (0.75) quartiles for all contamination profiles. The box has bars to show the maximum and minimum values of the flashover voltage gradient for each contamination profile. Figure 20 shows the variation range of the flashover voltage gradient which can provide useful information for understanding the conditions of the insulator under different

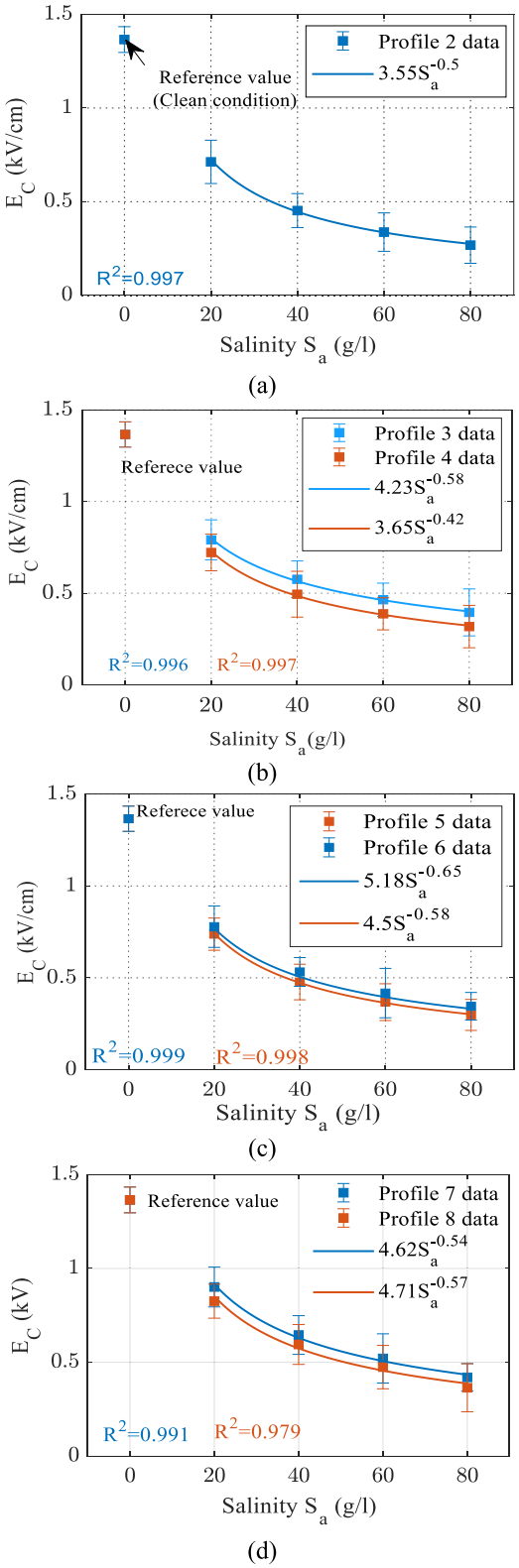

FIGURE 18. Flashover voltage stress of glass insulator under 75% humidity for different contamination profiles: (a) Profiles 1 and 2; (b) Profiles 3 and 4; (c) Profiles 5 and 6; (d) Profiles 7 and 8.

contamination profiles of distribution of contamination. It is observed that the Ec has the lowest median (Q (0.5) quartile) value of 0.39 kV/cm in contamination profile 2 which the

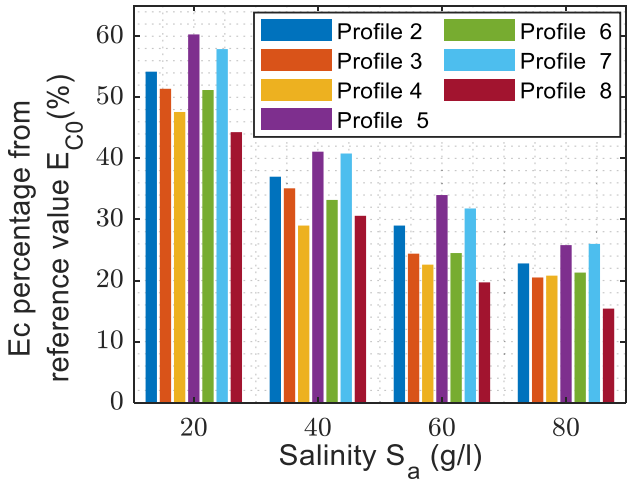

FIGURE 19. Percent of E_c from reference value E_{C0} for all contamination profile under different salinity and relative humidity of 75%.

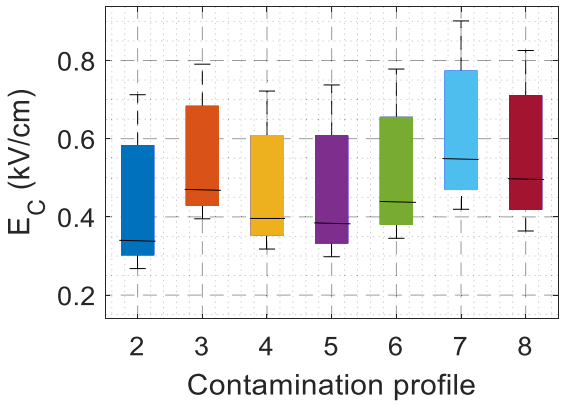

FIGURE 20. Flashover voltage gradient of the proposed contamination profiles under humidity of 75% and salinity from 20-80 g/l.

insulator in full pollution condition. This implies that as salinity grows, the insulator in these contamination profiles will reach the serious condition faster, and thus the probability of incidence of flashover increases exponentially. On the contrary, the highest median value for flashover voltage gradient values is in contamination profile 7 where only the top side of the insulator has pollution.

The operating voltage of the measured insulator corresponds to Ec value of 0.5 kV/cm. Consequently, from Figure 20, it can be observed that the median value of Ec values in contamination profiles 2, 4, 5 and 6 are lower than 0.5 kV/cm, this indicates that the flashover occurs in medium and heavy salinity in an insulator under operating voltage. Meanwhile, heavy salinity pollution based on contamination profiles 3, 7 and 8 that have a median value of more than 0.5 kV/cm causes the flashover problem based on experimental results.

B. EFFECT OF HUMIDITY ON FLASHOVER VOLTAGE

The humidity has a significant effect on flashover voltage of polluted insulators. The moisture impact under proposed

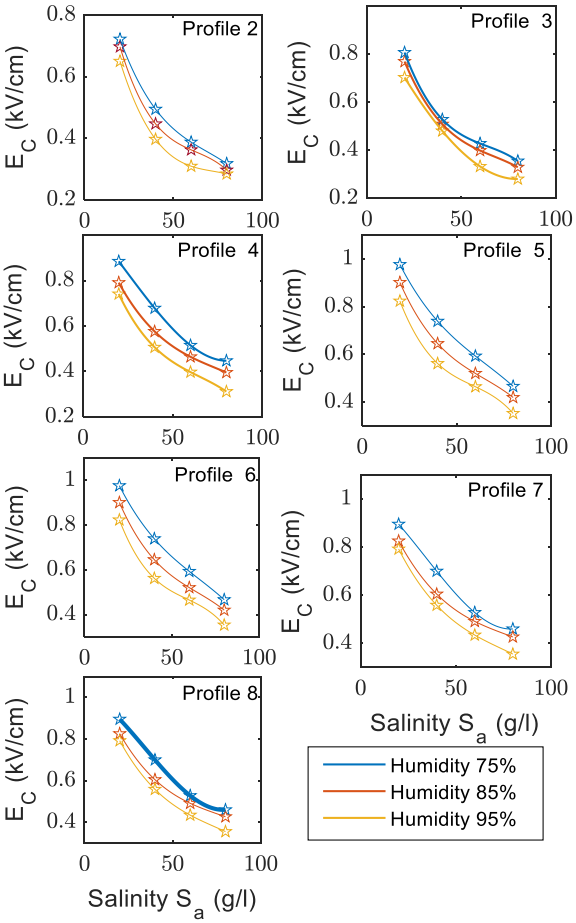

FIGURE 21. Flashover voltage gradient E_c of glass insulator for the proposed contamination profiles under different relative humidity.

scenarios for pollutant distribution is discussed in this section. Accordingly, three humidity levels have been selected which are 75%, 85%, and 95% to study this effect. Figure 21 shows the relationship between the flashover voltage gradient E_c and salinity levels with different humidity conditions. It can be concluded from Figure 21 that the relative standard of all experiment results does not exceed 5%, which indicates the experimental performance is effective. The result showed that the increase in humidity has an impact on the flashover voltage by decreasing its value. The influence of humidity varies from point to point, but humidity in general has significantly contributed by increasing the probability of incidence of flashover. For example, in contamination profile 5 with salinity equivalent to 40 g/l, the E_c of insulator which is humidified by 75%, 85% and 95%, decreased by 0.075 kV/cm and 0.153 kV/cm, respectively. Generally, the decrease in Ec–Sa line slope with the rise in relative humidity for contaminated insulators at contamination profiles 2–8 is roughly close to the contamination profile 5 slope with some oscillations in some cases that can be due to ambient circumstances.

V. CONCLUSION

The numerical simulation and experimental investigation were conducted on glass insulators under various pollution

and humidity levels. This investigation was performed using eight different distributions of contamination profiles. The numerical simulations of electrical potential, E-Field, and power dissipation were modelled for proposed contamination profiles. The effect of the dry band according to the proposed contamination profiles on potential and electric field distribution on the insulator surface was considered. Under the proposed contamination profiles, the increase in range of maximum electric field was found to be between 3% and 29%. The region of thermal hot spots appeared to be growing with a rise in the amount of contamination level in the region that is close to the electrodes of the insulator. Based on test results, it can be concluded that the flashover voltage gradient decreases with an increase in the salinity on the insulator surface. An increase in salinity (from 20 g/L to 80 g/L) decreases the flashover voltage gradient (within 0.73–1.1 kV/cm). Whereas, the insulator with full pollution had a lower value of flashover voltage gradient compared to other contamination profiles. Under certain salinity, that is 80 g/L, the increase in humidity (from 75% to 95%) resulted in reduction of the flashover voltage gradient for all contamination profiles (within 0.08–0.27 kV/cm). From the study carried out in this paper it can be concluded that the use of glass insulators under pollution either all-covered or in the presence of a dry band has an effect on the performance of the insulators and instability of the insulation system used on the transmission lines.

REFERENCES

[1] A. A. Salem, R. Abd-Rahman, S. A. Al-Gailani, Z. Salam, M. S. Kamarudin, H. Zainuddin, and M. F. M. Yousof, "Risk assessment of polluted glass insulator using leakage current index under different operating conditions," *IEEE Access*, vol. 8, pp. 175827–175839, 2020.

[2] Z. Zhang, X. Liu, X. Jiang, J. Hu, and D. W. Gao, "Study on AC flashover performance for different types of porcelain and glass insulators with non-uniform pollution," *IEEE Trans. Power Del.*, vol. 28, no. 3, pp. 1691–1698, Jul. 2013.

[3] W. Sima, T. Yuan, Q. Yang, K. Xu, and C. Sun, "Effect of non-uniform pollution on the withstand characteristics of extra high voltage (EHV) suspension ceramic insulator string," *IET Gener., Transmiss. Distrib.*, vol. 4, no. 3, pp. 445–455, 2010.

[4] X. Qiao, Z. Zhang, X. Jiang, and D. Zhang, "Contamination characteristics of typical transmission line insulators by wind tunnel simulation," *Electr. Power Syst. Res.*, vol. 184, Jul. 2020, Art. no. 106288.

[5] A. A. Salem, R. Abd-Rahman, S. A. Al-Gailani, M. S. Kamarudin, H. Ahmad, and Z. Salam, "The leakage current components as a diagnostic tool to estimate contamination level on high voltage insulators," *IEEE Access*, vol. 8, pp. 92514–92528, 2020.

[6] Z. Zhang, D. Zhang, W. Zhang, C. Yang, X. Jiang, and J. Hu, "DC flashover performance of insulator string with fan-shaped non-uniform pollution," *IEEE Trans. Dielectr. Electr. Insul.*, vol. 22, no. 1, pp. 177–184, Feb. 2015.

[7] A. A. Salem, R. Abd-Rahman, S. A. Al-Gailani, M. S. Kamarudin, N. A. Othman, and N. A. M. Jamail, "Artificial intelligence techniques for predicting the flashover voltage on polluted cup-pin insulators," in *Emerging Trends in Intelligent Computing and Informatics* (Advances in Intelligent Systems and Computing). Johor, Malaysia: Springer, 2020, pp. 362–372.

[8] A. A. Salem, R. A. Rahman, M. S. Kamarudin, and N. A. Othman, "Factors and models of pollution flashover on high voltage outdoor insulators: Review," in *Proc. IEEE Conf. Energy Convers. (CENCON)*, Oct. 2017, pp. 241–246.

[9] J. D. Samakosh and M. Mirzaie, "Investigation and analysis of AC flashover voltage of SiR insulators under longitudinal and fan-shaped non-uniform pollutions," *Int. J. Electr. Power Energy Syst.*, vol. 108, pp. 382–391, Jun. 2019.

[10] E. M. Savadkoohi, M. Mirzaie, S. Seyyedbarzegar, M. Mohammadi, M. Khodsuz, M. G. Pashakolae, and M. B. Ghadikolaei, "Experimental investigation on composite insulators AC flashover performance with fan-shaped non-uniform pollution under electro-thermal stress," *Int. J. Electr. Power Energy Syst.*, vol. 121, Oct. 2020, Art. no. 106142.

[11] A. Ali, A. Nekahi, S. G. Mcmeekin, and M. Farzaneh, "Numerical computation of electric field and potential along silicone rubber insulators under contaminated and dry band conditions," *3D Res.*, vol. 7, no. 3, p. 25, Sep. 2016.

[12] B. F. Hampton, "Flashover mechanism of polluted insulation," *Proc. Inst. Electr. Eng.*, vol. 111, no. 5, pp. 985–990, 1964.

[13] E. C. Salthouse, "Initiation of dry bands on polluted insulation," *Proc. Inst. Electr. Eng.*, vol. 115, no. 11, pp. 1707–1712, 1968.

[14] R. Abd-Rahman, A. Haddad, M. S. Kamarudin, M. F. M. Yousof, and N. A. M. Jamail, "Dynamic modelling of polluted outdoor insulator under wet weather conditions," in *Proc. IEEE Int. Conf. Power Energy (PECon)*, Nov. 2016, pp. 610–614.

[15] M. Bouhaouche, A. Mekhaldi, and M. Teguar, "Improvement of electric field distribution by integrating composite insulators in a 400 KV AC double circuit line in Algeria," *IEEE Trans. Dielectr. Electr. Insul.*, vol. 24, no. 6, pp. 3549–3558, Dec. 2017.

[16] Z. Zhang, S. Yang, X. Jiang, X. Qiao, Y. Xiang, and D. Zhang, "DC flashover dynamic model of post insulator under non-uniform pollution between windward and leeward sides," *Energies*, vol. 12, no. 12, p. 2345, Jun. 2019.

[17] R. A. Rahman, N. Harid, and A. Haddad, "Stress control on polymeric outdoor insulators," in *Proc. 45th Int. Univ. Power Eng. Conf. (UPE)*, 2010, pp. 1–4.

[18] A. Ali, M. A. Mughal, A. Nekahi, M. Khan, and F. Umer, "Influence of single and multiple dry bands on critical flashover voltage of silicone rubber outdoor insulators: Simulation and experimental study," *Energies*, vol. 11, no. 6, p. 1335, May 2018.

[19] N. A. Othman, M. A. M. Piah, and Z. Adzis, "Contamination effects on charge distribution measurement of high voltage glass insulator string," *Measurement*, vol. 105, pp. 34–40, Jul. 2017.

[20] R. Anbarasan and S. Usa, "Electrical field computation of polymeric insulator using reduced dimension modeling," *IEEE Trans. Dielectr. Electr. Insul.*, vol. 22, no. 2, pp. 739–746, Apr. 2015.

[21] M. Asadpoor, "Simulation and measurement of the voltage distribution on high voltage suspension porcelain insulator string under pollution condition," *Int. J. Appl. Sci. Eng. Res.*, vol. 1, no. 1, pp. 165–175, Feb. 2012.

[22] F. A. Jamaludin, M. Z. A. Ab-Kadir, M. Izadi, N. Azis, J. Jasni, M. S. A. Rahman, and M. Osman, "Effect of RTV coating material on electric field distribution and voltage profiles on polymer insulator under lightning impulse," in *Proc. 34th Int. Conf. Lightning Protection (ICLP)*, Sep. 2018, pp. 1–6.

[23] I. Ahmadi-Joneidi, A. A. Shayegani-Akmal, and H. Mohseni, "Leakage current analysis of polymeric insulators under uniform and non-uniform pollution conditions," *IET Gener., Transmiss. Distrib.*, vol. 11, no. 11, pp. 2947–2957, 2017.

[24] A. A. Salem, R. Abd-Rahman, M. S. Kamarudin, H. Ahmad, N. A. M. Jamail, N. A. Othman, M. T. Ishak, M. N. R. Baharom, and S. Al-Ameri, "Proposal of a dynamic numerical approach in predicting flashover critical voltage," *Int. J. Power Electron. Drive Syst. (IJPEDS)*, vol. 10, no. 2, p. 602, Jun. 2019.

[25] *Artificial Pollution Tests on High-Voltage Ceramic and Glass Insulators to be Used on A.C. Systems*, 3rd ed., Standard IEC 60507, International Electrotechnical Commission, 2013.

[26] A. A. Salem and R. Abd-Rahman, "A review of the dynamic modelling of pollution flashover on high voltage outdoor insulators," *J. Phys., Conf. Ser.*, vol. 1049, no. 1, 2018, Art. no. 012019.

[27] A. A. Salem, R. Abd-Rahman, H. Ahmad, M. S. Kamarudin, N. A. M. Jamal, N. A. Othman, and M. T. Ishak, "A new flashover prediction on outdoor polluted insulator using leakage current harmonic components," in *Proc. IEEE 7th Int. Conf. Power Energy (PECon)*, Dec. 2018, pp. 413–418.

[28] A. A. Salem, R. A. Rahman, M. S. Kamarudin, N. A. Othman, N. A. M. Jamail, H. A. Hamid, and M. T. Ishak, "An alternative approaches to predict flashover voltage on polluted outdoor insulators using artificial intelligence techniques," *Bull. Electr. Eng. Informat.*, vol. 9, no. 2, pp. 533–541, Apr. 2020.

[29] M. El-Shahat and H. Anis, "Risk assessment of desert pollution on composite high voltage insulators," *J. Adv. Res.*, vol. 5, no. 5, pp. 569–576, Sep. 2014.

[30] B. Dong, Z. Zhang, N. Xiang, H. Yang, S. Xu, and T. Cheng, "AC flashover voltage model for polluted suspension insulators and an experimental investigation in salt fog," *IEEE Access*, vol. 8, pp. 187411–187418, 2020.
[31] S. Nandi and B. S. Reddy, "Transient electric field analysis for polluted composite insulators under HVDC stress," *IEEE Trans. Power Del.*, early access, Apr. 16, 2020, doi: 10.1109/TPWRD.2020.2987143.
[32] J. Mahmoodi, M. Mirzaie, and A. A. Shayegani-Akmal, "Surface charge distribution analysis of polymeric insulator under AC and DC voltage based on numerical and experimental tests," *Int. J. Electr. Power Energy Syst.*, vol. 105, pp. 283–296, Feb. 2019.

ALI AHMED SALEM (Member, IEEE) received the M.Eng. degree in electrical power engineering from University Tun Hussein Onn Malaysia (UTHM), in 2016, where he is currently pursuing the Ph.D. degree in High Voltage with the Faculty of Electrical Engineering. His research interests include the dynamic arc modeling of pollution flashover on high voltage outdoor insulators.

R. ABD-RAHMAN (Member, IEEE) received the M.Eng. degree in electrical and electronics and the Ph.D. degree in high voltage from Cardiff University, U.K., in 2008 and 2012, respectively. He is currently a Senior Lecturer with the Faculty of Electrical and Electronic Engineering, Universiti Tun Hussein Onn Malaysia (UTHM). His research interests include dielectric materials, outdoor insulator, and discharge phenomenon. He is a Chartered Engineer U.K (C.Eng.) and a member of engineering institution such as the IET (MIET) and the Board of Engineers Malaysia (BEM).

WAN RAHIMAN received the bachelor's degree from Cardiff University, U.K., specializing in manufacturing engineering, and the Ph.D. degree in the field of fault detection and isolation for pipeline systems, in 2009. He is currently pursuing the Ph.D. degree with the Control System Centre, University of Manchester. He was an Engineer at Panasonic Manufacturing Ltd., Cardiff, and Lotus Cars Ltd., Norwich, for several years. He is currently a Senior Lecturer with the School of Electrical and Electronic Engineering, Universiti Sains Malaysia (USM), Engineering Campus, Penang, Malaysia. At USM, he serves as the Head of Cluster of Smart Port and Logistic Technology (COSPALT). His research interests lie in the area of modeling nonlinear systems on range of development research projects, particularly, in drone and autonomous vehicle technologies.

SAMIR AHMED AL-GAILANI received the B.Sc. degree from the Higher Technical Institute, Aden, Yemen, in 1992, and the Ph.D. degree in the field of optoelectronics from the University Technology Malaysia (UTM), in 2014, with Best Student Award. Since then, has been given various responsibilities, including teaching, postdoctoral fellow, supervising laboratory sessions, supervising postgraduate students and undergraduate students, academic advisor, head of laboratory, head of research group, chairman and member of different committees, as well as conducting short courses and training. He started his career as a Senior Lecturer at the Higher Technical Institute. He has authored 20 ISI articles and has an H-index of seven and total citations of 212, and has presented more than 90 papers in reputed refereed conferences. He also successfully supervised nine undergraduate students.

SALEM MGAMMAL AL-AMERI received the B.Eng. degree in mechatronics engineering from Asia Pacific University (APU), in 2012, the M.Eng. degree in electrical from Universiti Tun Hussein Onn Malaysia (UTHM), in 2016, and the Ph.D. degree from The Universiti Tun Hussein Onn Malaysia, in 2020. He is currently with the Universiti Tun Hussein Onn Malaysia Grantee for a postdoctoral position. His research interest includes transformers condition monitoring.

MOHD TAUFIQ ISHAK received the B.Eng. degree in electrical engineering from Universiti Tenaga Nasional, Malaysia, in 2002, the M.Eng. degree in electrical engineering from UMIST, U.K., in 2004, and the Ph.D. degree in electrical power engineering from the University of Manchester, U.K., in 2010. He is currently a Senior Lecturer with the Department of Electrical and Electronic Engineering, Universiti Pertahanan Nasional Malaysia. His research interests are high voltage, power transformer, asset management, lifetime prediction, renewable energy, conditioning monitoring, and smart grid.

USMAN ULLAH SHEIKH received the B.Eng. degree in electrical and mechatronics engineering, the M.Eng. degree in telecommunications engineering, and the Ph.D. degree in image processing and computer vision from Universiti Teknologi Malaysia, in 2003, 2005, and 2009, respectively. His research work is mainly on computer vision and embedded systems design. He is currently a Senior Lecturer with Universiti Teknologi Malaysia, working on image processing for intelligent surveillance systems. He is a member of the IET and has published works in many IEEE conferences.